

Synthesis and Characterization of Hydrotalcite-like Compounds Containing V³⁺ in the Layers and of Their Calcination Products

F. M. Labajos,[†] V. Rives,^{*,†} P. Malet,[‡] M. A. Centeno,[‡] and M. A. Ulibarri[§]

Departamento de Química Inorgánica, Universidad de Salamanca, Salamanca, Spain,
Departamento de Química Inorgánica e Instituto de Ciencia de Materiales,
Universidad de Sevilla-CSIC, Sevilla, Spain, and Departamento de Química
Inorgánica e Ingeniería Química, Universidad de Córdoba, Córdoba, Spain

Received July 7, 1995[⊗]

The synthesis and full characterization of a new hydrotalcite-like compound with the formula [Mg_{0.71}V_{0.29}(OH)₂](CO₃)_{0.145}·0.72H₂O and with V³⁺ in the layers are described. The influence of hydrothermal treatment and drying rate on the crystallinity of the materials obtained is discussed. The evolution to mixed oxides upon calcination at different temperatures (448, 548, 773, 1023, and 1273 K) under different atmosphere environments (air or nitrogen) for 2 h has been studied. Characterization of the original layered materials and of the calcination products has been carried out by X-ray diffraction, thermal analysis, Fourier-transform infrared spectroscopy, BET specific surface area determination, temperature-programmed reduction, and transmission electron microscopy. X-ray absorption spectroscopies (XANES and EXAFS) have also been used to assess the local geometry of vanadium ions in the different compounds prepared. All experimental data agree with a well-crystallized hydrotalcite-like compound after thermal treatment, and also a minor effect of the drying rate on the crystallinity has been found. Thermal decomposition yields poorly crystalline layered compound at 448 K that undergoes transformation to mostly amorphous materials when calcined at 548–773 K, finally leading to a mixture of MgO and Mg₃V₂O₈, which has increasing crystallinity as the calcination temperature increases. XAS results indicate the presence of V³⁺ ions in an octahedral coordination in the parent sample calcined at 448 K and tetrahedrally coordinated V⁵⁺ species for samples calcined at higher temperatures, calcination giving rise to a better ordering of the second coordination sphere. Similar results were found when calcination was performed in nitrogen, although higher temperatures were needed to achieve the same result.

Introduction

Double-layered hydroxides with the hydrotalcite structure are bidimensional basic solids of great importance in several chemical processes catalyzed by bases, as well as for treatment of wastes and also in medicine, owing to their absorbing ability and their suitability for anionic exchange. A large number of compounds with this structure are known in the two polytopic forms 3R and 2H, and a review on their synthesis, characterization, and properties has been published recently.¹ A preliminary report on the synthesis of a new compound with the hydrotalcite-like structure, possessing Mg²⁺ and V³⁺ ions in the brucite-like layers, has been described by us.² The importance of this compound comes from the fact that V³⁺ becomes stabilized in these layers and it provides a unique example of a precursor for mixed magnesium and vanadium oxides to be used in oxidation and dehydrogenation of alkanes.^{3–5}

Experimental Section

Synthesis of the Compounds. The compound was synthesized as described in ref 2, following the so-called constant-pH method, and

using Schlenk techniques.⁶ A 200 mL portion of a solution containing VCl₃ (0.5 M) and MgCl₂·6H₂O (1 M) was added dropwise to 250 mL of a solution containing Na₂CO₃·10H₂O (0.8 M) and NaOH (2.8 M). The system was maintained in flushing nitrogen at room temperature and atmospheric pressure. Water used to prepare the solutions had been deoxygenated and decarbonated by boiling and bubbling nitrogen while being cooled to room temperature. Addition of the solution containing the metallic cations to the basic solution extended along 2 h. Afterward, the suspension was magnetically stirred, and then the volume was reduced to 50% of the original volume by suction with a water pump. Two different sets of samples were prepared from the parent suspension. The solid was separated by centrifugation and washed until no evidence of chloride and Na⁺ was found in the washing liquids and then dried in an oven, at open air, at ca. 350 K (sample MgV-0A) or in a vacuum desiccator with anhydrous CaCl₂ (sample MgV-0B). Another set of samples were obtained by hydrothermal treatment of the suspension at 400 K for 7 or 18 days (samples MgV-I and MgV-II, respectively) in a stainless steel digestion bomb lined with Teflon. After washing to remove any traces of chloride and Na⁺ ions, both samples MgV-I and MgV-II were dried in a vacuum desiccator with anhydrous CaCl₂.

Characterization. Chemical analysis for magnesium and vanadium was carried out by atomic absorption in a Mark-II ELL-240 instrument. Analysis for C and H was performed in a Perkin-Elmer 2400 CHN apparatus. X-ray diffraction (XRD) patterns were recorded on a Siemens D-500 diffractometer with a graphite-filtered Cu Kα1 radiation (1.5405 Å, 1 nm = 10 Å) and interfaced to a DACO-MP data acquisition microprocessor provided with Diffract/AT software. Differential thermal analysis (DTA) and thermogravimetric analysis (TG) of the samples were carried out in Perkin-Elmer DTA 1700 and TGS-2 apparatuses, respectively, coupled to a Perkin-Elmer 3600 data station, at a heating rate of 10 K/min. Specific surface areas were measured

* To whom correspondence should be addressed. Fax +34 23 29 45 15.
E-mail: vrives@gugu.usal.es.

[†] Universidad de Salamanca.

[‡] Universidad de Sevilla.

[§] Universidad de Córdoba.

[⊗] Abstract published in *Advance ACS Abstracts*, January 15, 1996.

- (1) Cavani, F.; Trifiro, F.; Vaccari, A. *Catal. Today* **1991**, *11*, 173.
- (2) Rives, V.; Labajos, F. M.; Ulibarri, M. A.; Malet, P. *Inorg. Chem.* **1993**, *32*, 5000.
- (3) Chaar, M. A.; Patel, D.; Kung, M. C.; Kung, H. H. *J. Catal.* **1987**, *105*, 483.
- (4) Sien Hew Sam, D.; Soenen, V.; Volta, J. C. *J. Catal.* **1990**, *125*, 417.
- (5) Xingtao, G.; Ruiz, P.; Qin, X.; Xiexian, G.; Delmon, B. *J. Catal.* **1994**, *148*, 56.

(6) Shriver, D. F.; Drezdon, M. A. *The Manipulation of Air-Sensitive Compounds*, 2nd ed.; Wiley: New York, 1986.

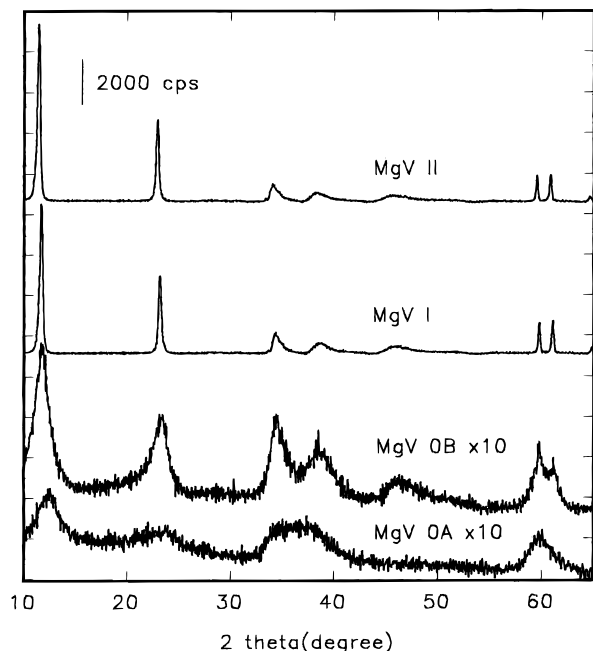


Figure 1. X-ray diffraction patterns of $\text{MgV}^{3+}/\text{CO}_3^{2-}$ hydrotalcite-like materials.

following the single-point method in a Micromeritics Flowsorb II-2300 apparatus by nitrogen adsorption after degassing the samples *in situ* at 400 K for 2 h. The Fourier-transform infrared spectra (FT-IR) of the samples were recorded in a Perkin-Elmer FT-IR 1730 apparatus, with a nominal resolution of 2 cm^{-1} and averaging 100 scans; the sample was pressed in KBr pellets.

Room temperature vanadium K-edge X-ray absorption spectroscopies (XAS) were recorded in transmission mode at station XAS-III at the LURE-DCI storage ring (Orsay, France). Monochromatization was achieved with a double-silicon crystal working at the (311) reflection. Energies were calibrated using a vanadium metal foil by setting its first peak in the derivative spectrum at 5465 eV. Analysis and handling of EXAFS spectra were carried out by using the program NEWEXAFS from the Eindhoven University of Technology. Experimental phase shift and backscattering amplitude functions for V–O were obtained from the spectra of Na_3VO_4 (bond length 1.69 Å, O/V coordination number 4.0).⁷ A V–V experimental reference, obtained from the EXAFS spectrum of a V foil, and theoretical functions obtained from FEFF were respectively used in the fit of V–V and V–Mg absorber–backscatter pairs. Standard deviations of fitted parameters were calculated for a noise level of 10^{-3} , being in general lower than estimated systematic errors in R ($\pm 1\text{--}3\%$) and N ($\pm 10\text{--}15\%$).

Temperature-programmed reduction (TPR) profiles were recorded in a conventional, homemade apparatus with catharometric detector using a 5% H_2/Ar mixture (from Sociedad Española del Oxígeno, S. A., Spain) as the carrier gas, with a flow of 50 mL/min and a heating rate of 10 K/min. Experimental conditions for TPR runs were chosen according to data reported elsewhere⁸ in order to attain good resolution of component peaks.

Transmission electron microscopy (TEM) was used to follow changes in the morphology of the samples with the thermal treatments. The photographs were obtained in a ZEISS-902 microscope, ultrasonically dispersing the solid in acetone.

Results and Discussion

Uncalcined Samples. The XRD patterns of the samples, Figure 1, show the profound effect of the hydrothermal treatment on the crystallinity degree of the solids obtained. Traces for samples MgV-I and MgV-II (hydrothermally treated) show peaks *ca.* 10 times more intense than those of samples MgV-

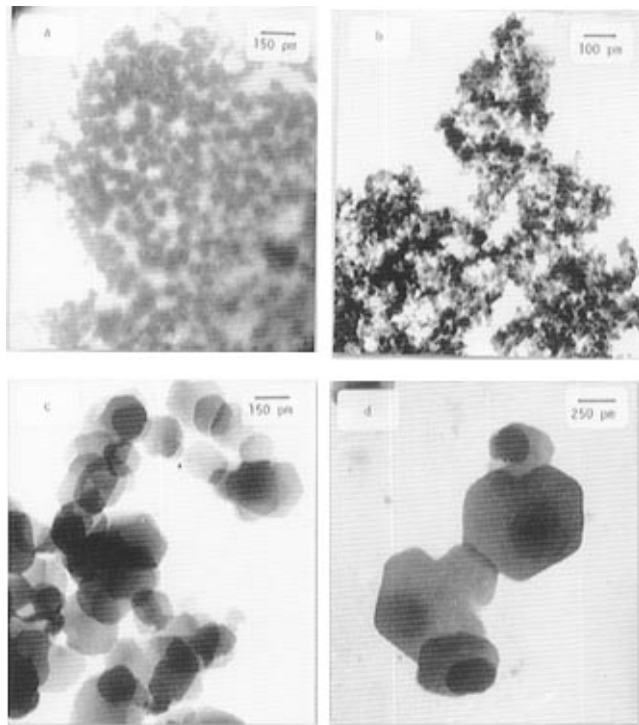


Figure 2. Transmission electron micrographs of samples: (a) MgV-0A; (b) MgV-0B; (c) MgV-I; (d) MgV-II.

OA and MgV-OB, dried in open air or in a desiccator, respectively (these traces have been expanded $\times 10$ in Figure 1). This effect is very much larger than that observed for similar compounds, also with the hydrotalcite-like structure without V^{3+} cations in the layers.⁹ Also, the drying process has an effect, although not so important as the hydrothermal treatment, on the crystallinity, as can be concluded from the sharpness of the most intense diffraction peaks for the samples dried in the vacuum desiccator as compared to those of the sample dried in open air.

XRD patterns for samples I and II are coincident (positions of the peaks and their relative intensities) with those reported for pure hydrotalcite.¹⁰ Lattice parameters, as calculated¹ from the positions of the peaks due to diffraction by planes (003), (006), and (009) for parameter c and (110) for parameter a , were 23.05 and 3.02 Å, respectively, for sample MgV-I and 23.43 and 3.04 Å, respectively, for sample MgV-II.

Transmission electron micrographs (TEM) in Figure 2 are consistent with conclusions from the XRD patterns. For sample 0A, Figure 2a, a set of nearly amorphous particles is observed, whose grain limits are hardly distinguished; a similar conclusion can be reached for sample 0B, Figure 2b, where the particles are extremely small, although their grain boundaries are better defined. On the contrary, micrographs for samples hydrothermally treated, Figure 2c,d, show well-defined crystals, hexagonal-shaped particles perfectly defined, with different intensities being due to overlapping of different particles as expected for lamellar compounds such as those studied here. These conclusions from XRD and TEM studies are consistent for a compound with a hexagonal cell ($a \approx 3\text{ Å}$) and periodicity along the c axis of three layers of hydroxyl groups in brucite-like layers. The OHs are stacking such that they form prisms between the lower and upper sheets of the consecutive brucite-like layers. This

(7) Tillmanns, E.; Baur, W. H. *Acta Crystallogr., Sect. B* **1971**, *27*, 2124.

(8) Malet, P.; Caballero, A. *J. Chem. Soc., Faraday Trans. 1* **1988**, *84*, 2369.

(9) Labajos, F. M.; Rives, V.; Ullibarri, M. A. *J. Mater. Sci.* **1992**, *27*, 1546.

(10) JCPDS: Joint Committee on Powder Diffraction Standards; International Centre For Diffraction Data: Swarthmore, PA, 1977.

Table 1. Chemical Analysis and Specific Surface Area Data for Samples Studied

sample	Mg ^a	V ^a	Mg:V ^b	C ^a	H ^a	(S _{BET}) ^c
MgV-0A	20.1	18.1	2.32	nm	nm	nm
MgV-0B	19.7	17.6	2.35	nm	nm	nm
MgV-I	19.7	16.9	2.45	1.9	3.2	22.0
MgV-II	20.0	16.9	2.48	1.8	3.2	19.6

^a % weight. ^b Atomic ratio. ^c m² g⁻¹. ^d nm = not measured.

polytype has been labeled by Bookin et al.^{11,12} as 3R1 and has rhombohedral symmetry, with the cations homogeneously distributed over the possible sites.

From XRD patterns, it is evident that samples MgV-I and MgV-II correspond to well-crystallized materials, and so, this study mainly corresponds to these two samples.

Table 1 shows the results of chemical analysis for the samples studied. Results are comparable for samples I and II, both with a well-defined hydrotalcite-like structure and with similar XRD patterns. On the other hand, the samples not submitted to hydrothermal treatment also show similar values for the chemical analysis, with a Mg:V atomic ratio of 2.3, slightly lower than that measured for the hydrothermally treated samples (2.47). This difference can be tentatively ascribed to a selective, partial removal of V³⁺ ions during the hydrothermal treatment, and whose presence introduces some sort of distortion in the structure that would decrease the stability of the lattice. The ionic radii for octahedrally coordinated Mg²⁺, Al³⁺, and V³⁺ are 0.86, 0.78, and 0.68 Å, respectively,¹³ and so, the presence of cations with different ionic radii (25% for Mg²⁺ and V³⁺) may introduce some sort of instability in the structure of the vanadium-containing brucite-like layer.

The specific surface area values, as determined by the single-point method, are also included in the same table, are rather similar for both samples submitted to hydrothermal treatment, and are of the same order as those previously measured for hydrotalcite-like materials submitted to hydrothermal treatment for a similar period of time.¹⁴ These values correspond to the external surface area, as diffusion of nitrogen molecules into the interlayer space is very slow.

Results from thermal analysis studies (DTA and TG) are summarized in Figure 3 for sample I; similar results were obtained for sample II. Curves were recorded in air and in nitrogen, leading to different profiles. These differences can thus be ascribed to oxidation processes during analysis in an oxidant atmosphere. The DTA profile, recorded in nitrogen, shows two endothermic effects with minima at 510 and 670 K, similar to those reported in the literature for hydrotalcite-like materials with nonoxidizable cations in the layers.^{9,15} The first effect is usually ascribed to removal of water molecules from the interlayer space, while the second peak, usually rather broad and, in some cases, with a clearly defined shoulder, is due to removal of hydroxyl groups from the brucite-like layers and removal of CO₂ from the interlayer carbonate anions. Both endothermic effects are recorded in the same temperature ranges

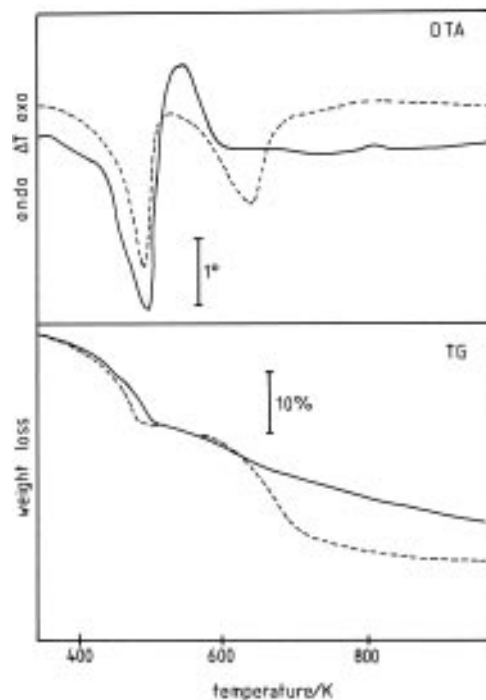


Figure 3. DTA and TG curves for sample MgV-I. Solid line: in air. Dotted line: in nitrogen.

where the TG profile shows two clearly different weight losses that correspond to 15 and 20%, respectively, of the initial sample weight.

The DTA and TG profiles recorded in air are rather similar to those recorded in nitrogen below *ca.* 540 K (i.e., just up to the end of the first endothermic effect/weight loss), thus suggesting that no oxidation process takes place in air below this temperature. A broad exothermic effect is recorded in the DTA curve with maxima at *ca.* 570 K, immediately after the first endothermic effect, while the second endothermic effect recorded under nitrogen is canceled. In addition, the TG profile shows a progressive weight loss, without any defined *plateau*. Also, the final weight loss is lower than that for the curve recorded in nitrogen. Such a difference is undoubtedly related to the oxidation of vanadium. The exothermic effect should correspond to energy release during oxidation of V³⁺, leading to a collapse of the structure, due to destruction of the brucite-like layers. In such a case, removal of the interlayer anions (carbonate, as carbon dioxide) and water (through condensation of hydroxyl from the layers) would take place in a fashion different from that observed during thermal decomposition of hydrotalcite-like materials where such an oxidation process does not take place (*vide infra*).

As noted above, evolution of the material up to *ca.* 540 K is identical under both atmospheres (air or nitrogen). Taking into account the weight loss up to this temperature, and the chemical analysis results in Table 1, the formula for samples MgV-I and MgV-II could be calculated as follows:

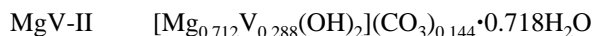
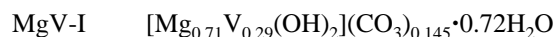


Figure 4 includes the FT-IR spectra of the samples. They are characteristic of hydrotalcite-like compounds containing carbonate counteranions in the interlayer. Spectra are almost coincident for both samples I and II. The intense peak at 3476 ± 4 cm⁻¹ is due to the OH stretching mode, its broadness

(11) Bookin, A. S.; Drits, V. A. *Clays Clay Miner.* **1993**, *41*, 551.

(12) Bookin, A. S.; Cherkasin, V. I.; Drits, V. A. *Clays Clay Min.* **1993**, *41*, 558.

(13) Huheey, J. E.; Keiter, E. A.; Keiter, R. L. *Inorganic Chemistry. Principles of Structure and Reactivity*, 4th ed.; Harper Collins: New York, 1993.

(14) Labajos, F. M.; Rives, V.; Ullibarri, M. A. In *Multifunctional Mesoporous Inorganic Solids*; Sequeira, C. A. C., Hudson, M., NATO-ASI, Eds.; Kluwer Academic Publishers: Dordrecht, The Netherlands, 1993; p 207.

(15) Pesic, L.; Salipurovic, S.; Markovic, V.; Vucelic, D.; Kagunya, W.; Jones, W. *J. Mater. Chem.* **1992**, *2*, 1069.

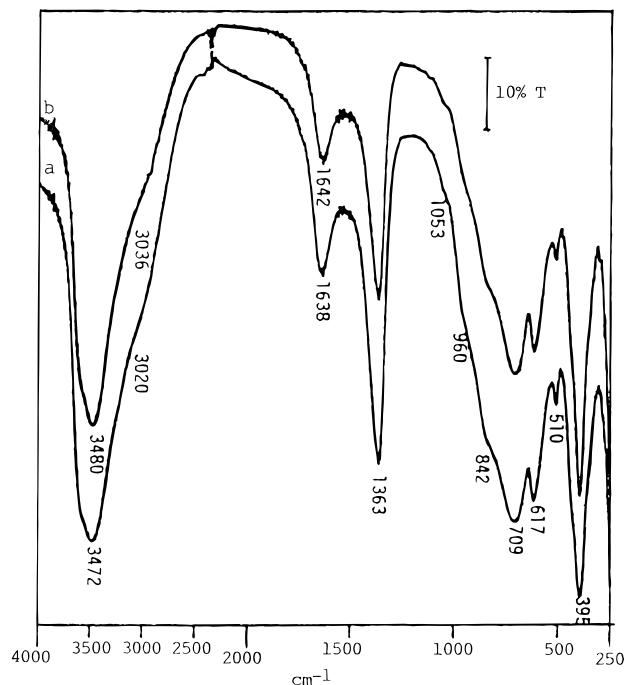


Figure 4. FT-IR spectra of samples (a) MgV-I; (b) MgV-II.

indicating the participation of these hydroxyl groups (both from the brucite-like layers and from the interlayer water molecules) in hydrogen bonding. The noticeable shoulder at $3028 \pm 8 \text{ cm}^{-1}$ is due to hydrogen bonding with the interlayer carbonate anions.¹⁶ The absorption at $1640 \pm 2 \text{ cm}^{-1}$ is due to mode $\delta_{\text{H}_2\text{O}}$ of interlayer water molecules. Bands originated by the carbonate anions are shifted with respect to the values reported for free carbonate. So, the ν_3 stretching mode band is recorded at 1363 cm^{-1} ; mode ν_2 gives rise to the band at 842 cm^{-1} , and the band originated by mode ν_4 is included in the absorption at 617 cm^{-1} . Even the band due to mode ν_1 can be hardly distinguished as a weak shoulder close to 1050 cm^{-1} ; although this mode is IR-forbidden for free carbonate, it becomes activated within the restricted symmetry in the interlayer space. Bands below *ca.* 800 cm^{-1} are due to metal–oxygen vibration modes.

The oxidation state and local coordination of vanadium ions in sample II were assessed by X-ray absorption spectroscopy.

As previously reported,² the V–K-edge XANES spectrum almost coincides with that reported by Wong et al.¹⁷ for roscoelite, a layered mineral in which the Al^{3+} ions in the octahedral $[\text{AlO}_6]$ sheets are partially substituted by V^{3+} . The location of V^{3+} cations in the layers of the hydrotalcite structure in an octahedral coordination is also assessed by analysis of the EXAFS oscillations at the V–K-edge, Figure 5. Thus, the associated Fourier transform (FT) shows a clear maximum at 1.7 \AA , uncorrected, that can be fitted by 5.91 ± 0.06 oxygen neighbors at $2.012 \pm 0.001 \text{ \AA}$, a distance characteristic of V^{3+} cations in octahedral coordination.¹⁷ Moreover, in the layered structure, V^{3+} cations are expected to have six cations as second-shell neighbors that would be responsible for the second maximum at 2.7 \AA in the uncorrected FT. Best fit of this second maximum is obtained by considering 5.85 ± 0.07 magnesium atoms at $3.113 \pm 0.001 \text{ \AA}$, in good agreement with the expected coordination number for the hydrotalcite structure and the *a* parameter of the crystal (*ca.* 3 \AA), as determined by XRD. Thus, XAS data confirm that most of vanadium ions in this sample are in an oxidation state of +3, and it confirms the isomorphic substitution of V^{3+} ions for Mg^{2+} ions in the octahedral sites of the brucite layers. It should be noted that the presence of only Mg^{2+} cations in the second coordination shell of vanadium suggests a nonrandom distribution of Mg^{2+} and V^{3+} ions in the layers, in such a way that trivalent cations do not occupy adjacent positions within the layers, thus minimizing electrostatic repulsions.¹⁸

Calcined Samples. As already mentioned, the Mg–V–O oxides are important as heterogeneous oxidation catalysts. In order to identify the stable phases formed during thermal decomposition of the MgV hydrotalcite-like materials studied in this work, we have carried out a detailed analysis of sample II after it was submitted to calcination in air under the following conditions. A portion of the sample was calcined in an open crucible in a Select-Horn furnace for 2 h at 448, 548, 773, 1023, and 1273 K, while a second portion was heated at the same temperatures and also for 2 h but in a tubular Heraeus ROK3/60 furnace, while flowing N_2 (50 mL/min), in order to obtain samples calcined in oxygen-free conditions. In order to ensure an oxygen-free atmosphere during calcination, the sample was flushed with nitrogen for 15 min prior to calcination and during the cooling to room temperature.

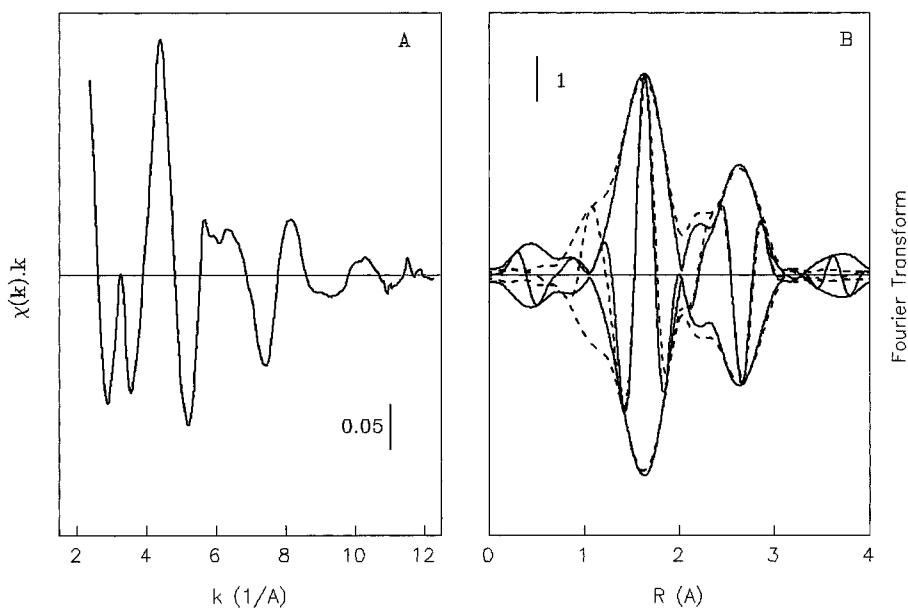


Figure 5. (A) Unfiltered EXAFS oscillations at the V–K-edge for sample II. (B) Absolute and Imaginary parts of the associated k^3 -weighted Fourier transform ($\Delta k = 3.44\text{--}12.00 \text{ \AA}^{-1}$). Solid lines: experimental data. Dashed lines: best fit functions.

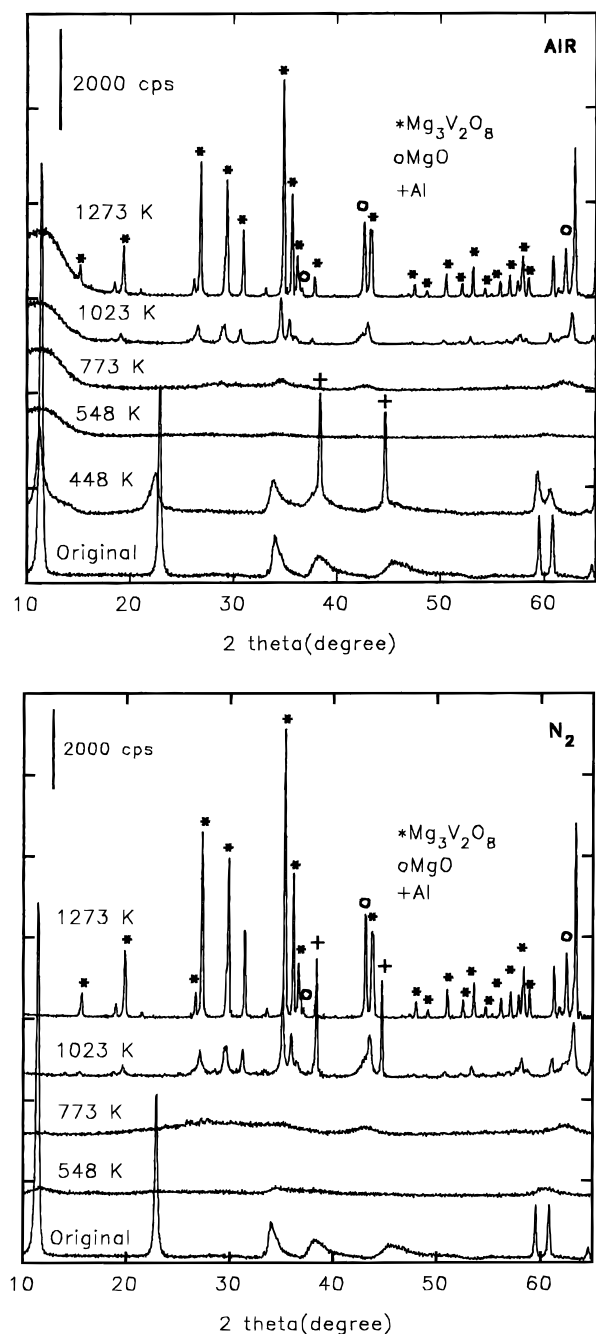


Figure 6. X-ray diffraction patterns of sample MgV-II calcined in air (a) and in nitrogen (b) at the temperatures given (peaks due to the Al sample holder were recorded in some cases).

The XRD patterns of the solids obtained after calcination in air and in nitrogen are given in Figure 6. Slight, although noteworthy, differences are observed, depending on the calcination atmosphere. When the sample is calcined at 448 K in air, the material retains its layered structure but with a lower crystallinity. A complete amorphous material is obtained when the sample is calcined in air at 548 K, although weak, broad peaks centered at 3.09, 2.64, and 1.53 Å can be hardly distinguished. When calcination is performed in nitrogen, the profile recorded corresponds to a solid with a collapsed structure in which there are some remaining layers.

As the calcination temperature is increased, the differences between the XRD diagrams of samples calcined in air and in nitrogen become narrower. Therefore, after calcination at 773 K, the XRD diagram shows only broad features due to MgO. When the calcination temperature is raised above 1000 K, the peaks recorded are associated (file 19-779 in ref 10) with MgO and, mainly, with $\text{Mg}_3\text{V}_2\text{O}_8$, although these peaks are still rather weak for the sample calcined at 1023 K but are well-defined in the XRD diagram of the sample calcined at 1273 K. It can be mentioned, however, that peaks are sharper (i.e., corresponding to better crystallized solids) when the sample is calcined in nitrogen, probably due to the lower cooling time required when calcination is carried out in air, thus leading to sinterized particles (larger size, sharper XRD peaks) on calcining in nitrogen (a larger cooling time was required in the tubular furnace, before removing the nitrogen flow). Similar XRD profiles have been reported by Kung et al.³ and Delmon et al.⁵ for Mg–V–O catalysts obtained using other synthetic methods.

The evolution of the specific surface area values with the calcination temperature is in agreement with the crystallinity degree of the samples derived from XRD. The well-crystallized starting compound has a specific surface area of $19 \text{ m}^2 \text{ g}^{-1}$; this value remained constant after calcination at 448 K. Thermal treatments at 548 and 773 K led to a collapse of the structure, yielding amorphous compounds with an increase in the specific surface area value, reaching a value of $26 \text{ m}^2 \text{ g}^{-1}$. Upon calcination at 1023 K, the sample shows a decrease in the value of its specific surface area, $16 \text{ m}^2 \text{ g}^{-1}$, as the result of the formation of the crystallized mixed oxide phase determined by XRD. An increase in the calcination temperature led to a dramatic decrease in the specific surface area; thus after calcination at 1273 K, treatment that yields a well-defined mixed magnesium–vanadium oxide, the specific surface area was only $4 \text{ m}^2 \text{ g}^{-1}$.

The FT-IR spectra recorded for the calcined products show an evolution similar to (with respect to the effect of the calcination atmosphere) that reported above from the XRD patterns. Bands due to modes originated by hydroxyl and carbonate groups are recorded for samples calcined below 773 K. The intensity of the shoulder at *ca.* 3020 cm^{-1} (due to ν_{OH} of OH groups hydrogen-bonded to carbonate species) decreases as the calcination temperature increases (below 773 K), as does the band close to 1630 cm^{-1} due to the presence of molecular water. The ν_3 mode of carbonate splits into two peaks at 1540 and 1420 cm^{-1} after calcination at 548 and 773 K. Such a splitting can be explained on the basis of a lower symmetry of the carbonate species,¹⁶ although the positions of these peaks are closer to those of alkaline earth carbonates,¹⁹ thus suggesting that these type of salts are probably formed during breakdown of the layered structure. However, as its presence has not been confirmed by XRD, it should be concluded that they are very well-dispersed (i.e., amorphous).

As expected, the FT-IR spectra for the samples calcined at or above 1000 K are absolutely different. Those for the sample calcined in air at 1023 and 1273 K are given in Figure 7, and the assignment of the peaks for the sample calcined at 1273 K is summarized in Table 2. Most of them are due to bands already reported²⁰ for tetrahedral $[\text{VO}_4]$ species, although other bands (whose positions are not given in the table) are originated by MgO.²¹ The positions of the bands due to V-containing

(16) Hernandez-Moreno, M. J.; Ulibarri, M. A.; Rendon, J. L.; Serna, C. *J. Phys. Chem. Miner.* **1985**, *12*, 34.
 (17) Wong, J.; Lytle, F. W.; Messmer, R. P.; Maycotte, D. H. *Phys. Rev. B* **1984**, *30*, 5596.
 (18) Malet, P.; Odriozola, J. A.; Labajos, F. M.; Rives, V.; Ulibarri, M. A. *Nucl. Instrum. Methods Phys. Res., Sect. B* **1995**, *97*, 16.

(19) Ulibarri, M. A.; Cornejo, J.; Hernandez, M. J. *J. Mater. Sci.* **1987**, *22*, 1168.
 (20) Hanuza, J.; Jezowska-Trzebiatowska, B.; Oganowski, W. *J. Mol. Catal.* **1985**, *29*, 109.
 (21) Nyquist, R. A.; Kagel, R. O. *Infrared Spectra of Inorganic Compounds*; Academic Press: New York, 1971.

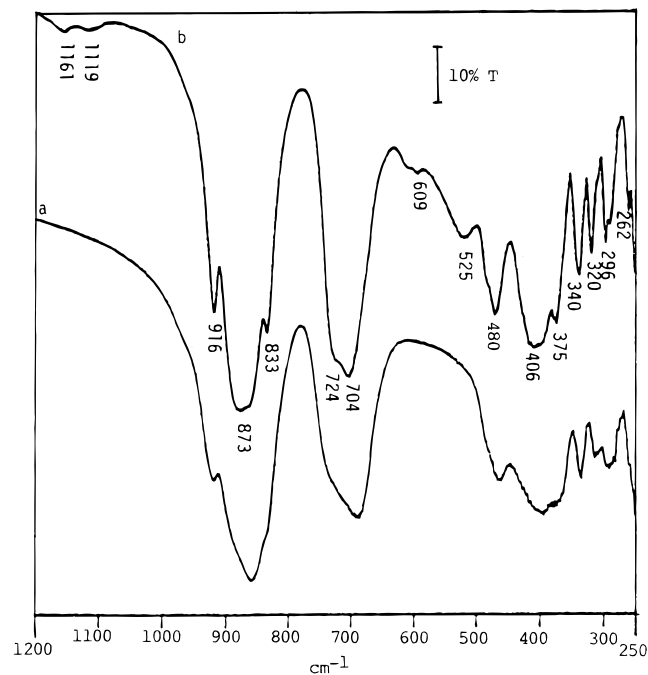


Figure 7. FT-IR spectra of products obtained after calcination of sample MgV-II in air at (a) 1023 and (b) 1273 K.

Table 2. Assignment of the Most Important FT-IR Peaks Recorded in the FT-IR Spectrum of Sample MgV-II Calcined at 1273 K (1200–250 cm^{-1} Range)

position/ cm^{-1}	ascription
916	$\nu_s(\text{VO}_4)$
873	$\nu_{as}(\text{VO}_4)$
833	
704	$\nu_{as}(\text{VOV})$
480	$\nu_s(\text{VOV})$
469	$\delta_s(\text{VO}_4)$
406	
375	
340	$\delta_{as}(\text{VO}_4)$
320	
296	
291	
262	

species are very close to those reported by Hanuza et al.²⁰ for magnesium *ortho*-vanadate and also to those of oxides (mostly containing $\text{Mg}_3\text{V}_2\text{O}_8$) reported by Kung et al.³ and Delmon et al.⁵

XRD and FT-IR data show that V^{3+} cations in the original hydrotalcite are oxidized to V^{5+} after heating the sample at temperatures higher than 1000 K. A well-defined $\text{Mg}_3\text{V}_2\text{O}_8$ phase is identified under these conditions. However, samples with the highest specific surface area and with the highest interest as catalytic materials are formed after thermal treatments at temperatures below 1000 K. These materials are amorphous and, since neither the oxidation degree of vanadium cations nor the nature of the vanadium compounds formed are inferred from XRD and FT-IR data, they have been studied by X-ray absorption spectroscopy. The XANES spectrum (Figure 8A) of a sample calcined at 448 K is identical to that recorded for the uncalcined samples, indicating that vanadium cations mainly remain as V^{3+} species in the layers of the hydrotalcite structure. On the other hand, for the sample calcined at 1273 K (where XRD undoubtedly detects crystalline $\text{Mg}_3\text{V}_2\text{O}_8$), the high intensity of the pre-edge peak is associated¹⁷ with the oxidation state +5 for vanadium ions. As shown in Figure 8 for samples calcined at 548–1023 K, both the intensity of the pre-edge peak and the structure of post-edge features indicate that in the

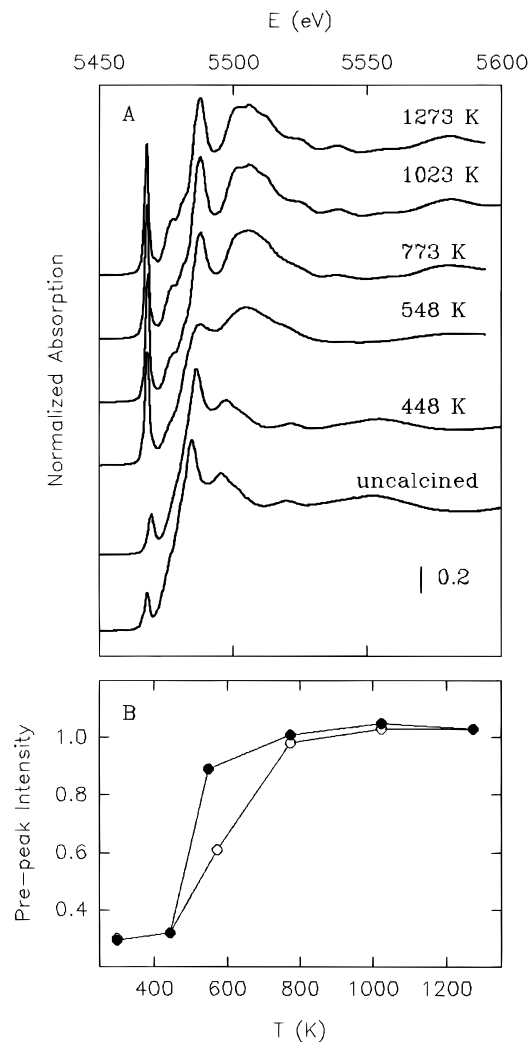


Figure 8. (A) V-K-edge XANES spectra of sample MgV-II as prepared and after calcination in air at 448–1273 K. (B) Intensities of the pre-edge peak as a function of the calcination temperature in air (filled circles) and in nitrogen (open circles).

amorphous materials vanadium ions are mainly in the +5 oxidation state, and in a local surrounding similar to that found in $\text{Mg}_3\text{V}_2\text{O}_8$. Normalized intensities of the pre-edge peak (Figure 8B) indicate that oxidation of vanadium is complete after heating at temperatures equal to or above 773 K under either air or N_2 , while the sample heated at 548 K is not fully oxidized, the oxidation degree of vanadium being considerably lower for the sample heated under nitrogen.

EXAFS data at the V-K-edge for the calcined samples (Figure 9) provide a more detailed picture of the local surrounding of vanadium cations in the calcined materials. In agreement with previous conclusions, the associated k^1 -weighted FT spectra show a first maximum that is independent of the calcination temperature, indicating that the first coordination shell of V^{5+} in the amorphous materials is identical to that found in crystalline $\text{Mg}_3\text{V}_2\text{O}_8$, where vanadium atoms are forming tetrahedral $[\text{VO}_4]$ units.²² Best fit parameters for this first-shell maximum are given in Table 3, confirming the tetrahedral coordination of V^{5+} cations by oxygen atoms at *ca.* 1.70 Å in these samples. An increase in the calcination temperature leads to the development of a second coordination shell, at *ca.* 3 Å in the uncorrected FT, that is absent in the sample calcined at 448 K and reaches its maximum intensity for samples calcined

(22) Krishnamachari, N.; Calvo, C. *Can. J. Chem.* **1971**, *49*, 1629.

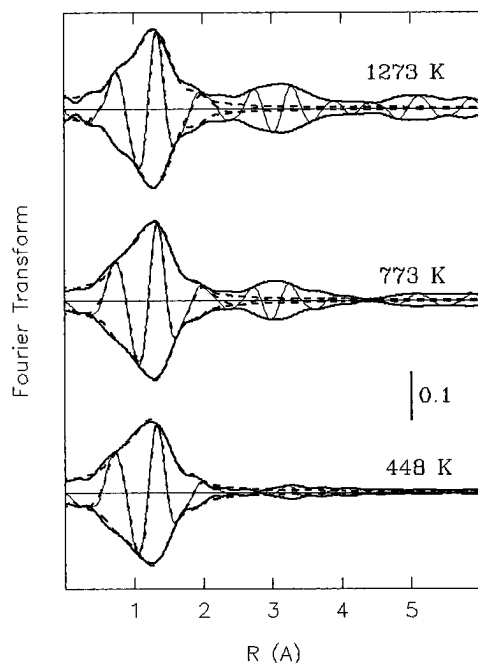


Figure 9. Absolute and imaginary parts of the associated k^1 -weighted Fourier transforms of V–K-edge EXAFS oscillations for sample MgV-II calcined in air at 548–1273 K. Solid lines: experimental data. Dashed lines: best fit functions for the first oxygen shell ($\Delta k = 3.5$ – 12.0 \AA^{-1} in all the Fourier transforms).

Table 3. Best Fit Parameters for the First Coordination Shell in Calcined Sample MgV-II^a

T (K)	N	R (\AA)	$\Delta\sigma^2 \times 10^3$ (\AA^{-2})	ΔE^o (eV)
448	3.72 ± 0.03	1.691 ± 0.001	2.9 ± 0.1	-0.2 ± 0.1
773	3.85 ± 0.03	1.719 ± 0.001	1.7 ± 0.1	-3.0 ± 0.1
1023	4.05 ± 0.03	1.716 ± 0.001	1.6 ± 0.1	-3.1 ± 0.1
1273	3.41 ± 0.03	1.719 ± 0.001	1.7 ± 0.2	-3.7 ± 0.2

^a Standard deviations are given for a noise level 10^{-3} in $\chi(k)$. Values are always lower than estimated systematic errors ($\pm 0.02 \text{ \AA}$ in bond distance, R , and $\pm 15\%$ in coordination number, N).

at $T \geq 1023 \text{ K}$. This second shell in crystalline $\text{Mg}_3\text{V}_2\text{O}_8$ is formed by oxygen, vanadium, and oxygen atoms at close distances (V 3.410 , $2 \times 3.712 \text{ \AA}$; O 2×3.222 , $10 \times 3.5 \pm 0.1 \text{ \AA}$; Mg 2×3.357 , $7 \times 3.46 \pm 0.02 \text{ \AA}$), and its complex structure prevented us from attempting its fitting. However, the increase in second-shell intensity with the calcination temperature suggests that vanadate nuclei already formed at 448 K steadily grow as the calcination temperature is increased, the second shell being already ordered as in the crystalline material after heating at 1023 K.

The ease by which vanadium (in the materials calcined at increasing temperatures) is reduced by H_2 was assessed by TPR. For all the samples, total hydrogen uptakes correspond to 1.0 H_2/V , indicating a full reduction from V^{5+} to V^{3+} during the TPR experiment. However, the TPR profile is affected by the calcination temperature (Figure 10). Thus, for the sample calcined at 1273 K, the onset of the reduction process as well as the position of its maximum are *ca.* 200 K higher than that in the materials calcined in the range 548–1023 K. The shift of the reduction processes to lower temperatures for materials

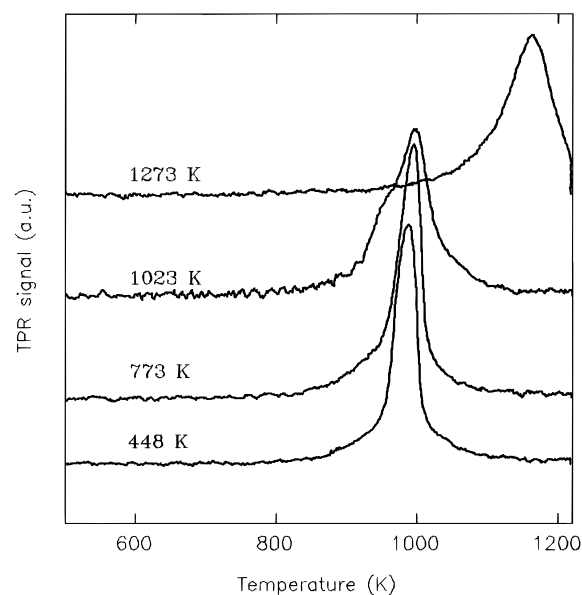


Figure 10. Temperature-programmed reduction profiles of sample MgV-II calcined in air at 548–1273 K.

that were previously calcined up to 1023 K indicates a significantly higher reactivity of vanadium atoms in these samples.

Conclusions

The solids obtained in this work are well-crystallized if submitted to hydrothermal treatment after precipitation. In these materials, V^{3+} ions are octahedrally coordinated in the brucite-like layers, carbonate anions existing in the interlayers. Local geometry and oxidation state of vanadium ions are confirmed by XAS.

Calcination above 448 K leads to oxidation of V^{3+} to V^{5+} ; such a process takes place even if calcination is carried out in nitrogen, although in this case higher temperatures are needed to attain the same result.

Amorphous solids with a high specific surface area are obtained when calcination is performed between 548 and 773 K. Crystallization of $\text{Mg}_3\text{V}_2\text{O}_8$ and MgO starts at 1023 K, finally forming well-crystallized materials upon calcination at 1273 K. The local surrounding of V^{5+} ions in the amorphous solids is the same as that in well-crystallized $\text{Mg}_3\text{V}_2\text{O}_8$. The increase in the calcination temperature gives rise to a steady ordering of the layers for longer distances, thus exclusively giving rise to a higher crystallinity, without any other effect.

Reducibility of vanadium ions in samples calcined at intermediate temperatures is easier than when the sample has been previously calcined at 1273 K, thus indicating a higher reactivity of V^{5+} species when calcination is performed at 548–1023 K.

Acknowledgment. Financial support from CICYT (MAT93-0787), DGICYT (PB92-0665), and Consejería de Cultura y Turismo de la Junta de Castilla y León is greatly acknowledged. The authors also thank Mr. A. Montero for measuring the specific surface areas of the samples.

IC9508350